

Maximum Entropy Framework for a Universal Rank Order distribution with Socio-economic Applications

Abhik Ghosh,¹ Preety Shreya,² and Banasri Basu²

¹*Interdisciplinary Statistical Research Unit, Indian Statistical Institute, Kolkata 700108**

²*Physics and Applied Mathematics Unit, Indian Statistical Institute, Kolkata 700108, India[†]*

(Dated: September 30, 2019)

In this paper we derive the maximum entropy characteristics of a particular rank order distribution, namely the discrete generalized beta distribution, which has recently been observed to be extremely useful in modelling many several rank-size distributions from different context in Arts and Sciences, as a two-parameter generalization of Zipf's law. Although it has been seen to provide excellent fits for several real world empirical datasets, the underlying theory responsible for the success of this particular rank order distribution is not explored properly. Here we, for the first time, provide its generating process which describes it as a natural maximum entropy distribution under an appropriate bivariate utility constraint. Further, considering the similarity of the proposed utility function with the usual logarithmic utility function from economic literature, we have also explored its acceptability in universal modeling of different types of socio-economic factors within a country as well as across the countries. The values of distributional parameters estimated through a rigorous statistical estimation method, along with the *entropy* values, are used to characterize the distributions of all these socio-economic factors over the years.

I. INTRODUCTION

The idea that mathematics and physics can illuminate human conduct dates back to the eighteenth century [1]. Later, it was proposed that there are general scientific laws describing human societies [2], and statistical analyses of human qualities began therefrom [3]. Today the sciences of sociophysics and econophysics draw on all these ideas in their attempts to explain the socio-economic behavior in societies. In modern use *social physics* refers to using *big data* analysis and the mathematical laws to understand the behavior of socio-economic patterns. The core idea is that the socio-economic data contain mathematical patterns that are characteristic of how social interactions spread and their converge. With the availability of huge amount of empirical data for a abundance of measures of human interactions makes it possible to divulge the socio-economic patterns. Finding the mathematical shape of a distribution function is as simple as a curve fitting but the significance of the mathematical form used to fit it should be clarified and explained. It is also important to know if the shape of a given distribution function can be explained by an underlying generative principle. Statistical physics plays a major role in this effort by bringing tools and concepts able to bridge theory and empirical results. In this respect, the principle of Maximum entropy (MaxEnt) from statistical physics [4] provides a natural tool for deriving many standard probability distributions [5]. Principles underlying power-law distributions have been sought in various types of models. In the present paper our focus is to formulate a Maximum entropy framework for a two-parameter Rank-Order (RO) distribution and show that the MaxEnt principle used in estimating probabilistic models from appropriate constraints is also the underlying basis of many socio-economic models via this universal RO distribution [6–12]. Our next goal is to characterize the uncertainty over the time span in the respective distributions through entropy analysis and study their evolution.

The rank order distributions are very useful in modeling several grouped or ungrouped socio-economic data where we can arrange (*rank*) the data-points or groups according to their importance (*size*). To model a variable based on N data-points (or groups) arranged in decreasing order of *importance* with i -th item having rank r_i and size n_i , the most commonly used RO distribution is the hyperbolic Pareto (Zipf's) law. It assigns a probability for ranks (r) by the probability mass function $f_P(r) = A \cdot r^{-\nu}$, for $r = 1, \dots, N$, where A is the normalizing constant and $\nu > 0$ is the scaling (exponent) parameter. This Pareto law has also seen to be the maximum entropy distribution under the restriction imposed in terms of the expected utility function, when we consider the popular logarithmic utility, $u(r) = \log(r)$, from standard economic literature [13]. However, as evident from several empirical applications, this Pareto or power law can yield a good fit to any empirical data-sets only at the end of low-ranks (large sizes) [14, 15]

*Electronic address: abhianik@gmail.com

[†]Electronic address: sribbasu@gmail.com

and fails miserably at the other end of the rank order distribution specially when the data exhibits a wider spectrum of rank-sizes [7].

As an alternative to the Pareto law, a recently developed RO distribution, namely the discrete generalized beta (DGB) distribution, proposed in [16, 17], is seen to provide much improved fits for a wider spectrum of rank size data arising from different areas of arts and science [6]. The probability mass function associated with the DGB distribution is defined in terms of two real scaling parameters (a, b) and is given by

$$f_{(a,b)}(r) = A \frac{(N+1-r)^b}{r^a}, \quad r = 1, \dots, N, \quad (1)$$

with A being the required normalizing constant. Several scientists have shown its successful applications in modelling different types of rank ordered data [6–12]. These also include the study of the social variable like city sizes [7] in discrete attempts but no extensive study is available considering different types of important socio-economic factors. Importantly, the underlying theory responsible for the success of this particular RO distribution is not explored properly. This paper is the first to provide a derivation of this particularly useful RO distribution as a natural maximum entropy distribution under the appropriate bivariate utility constraints. Moreover, our analysis will also illustrate its acceptability in universal modeling of different types of socio-economic factors. In particular, for validating our proposal we have considered data for diverse socio-economic factors within a country as well as across the countries.

The rest of the paper is organized as follows. Sec. II deals with the mathematical formulation of the Maximum Entropy Rank Order distribution. In Sec. III we validate our theoretical proposal with empirical data sets of different socio-economic variables within a country for a large time span. The discussion on the uncertainty of the distribution is also narrated with the help of the entropy of the corresponding distribution. The corresponding subsections A, B and C respectively deals with city sizes of Japan, personal and household income of USA and election results of India for various years. Furthermore, in Sec. IV we demonstrate our proposal with a few socio-economic indicators across different countries around the globe and do a comparative analysis in terms of entropy at different time points. The respective subsections A, B, and C of Sec IV illustrates the RO distribution and the corresponding Shannon entropies for the population, percentage of agricultural land, GDP per capita and Buffet indicators of different countries across the world. Finally, we conclude in Sec. V.

II. THE MAXIMUM ENTROPY RANK ORDER DISTRIBUTIONS

Although initially introduced for solving a problem in statistical mechanics [4], the principle of Maximum Entropy has become a widely applied tool for constructing the probability distribution in statistical inference, decision science, pattern-recognition, communication theory, time-series analysis, and many more. The function which is maximized, namely the entropy, does have remarkable properties entitling it to be considered a good measure of the amount of uncertainty contained in a probability distribution [18]. We point out here that currently MaxEnt is being regarded as a principle that is broader than either physics or information alone. It is also a procedure which ensures that any inference drawn from stochastic data satisfies the basic self-consistency requirements [19].

Let us consider an RO distribution having support $\{1, 2, \dots, N\}$; this can be used to model rank-size data on N items (data-points). Suppose we use a model which assigns the probabilities to different ranks through a probability mass function (pmf) $f(r)$, $r = 1, \dots, N$. Note that, by definition, it satisfies

$$\sum_{r=1}^N f(r) = 1. \quad (2)$$

As the uncertainty in any model distribution can be measured by the Shannon-Gibb's entropy, we use the distribution with maximum uncertainty (entropy) according to the Jaynes' MaxEnt principle [4]. The Shannon entropy of our model RO distribution $f(r)$ is given by

$$S(f) = - \sum_{r=1}^N f(r) \log f(r), \quad (3)$$

where the logarithm is taken with base e (natural logarithm). It is straightforward and intuitive to see that the pmf that maximizes the Shannon entropy in (3) subject to the normalizing constraints (2) is the uniform distribution [5] which assigns equal probability (of $\frac{1}{N}$) to each rank with the corresponding (global) maximum entropy value being $\log(N)$. In practice, however, no data are uniformly distributed and cannot be modelled by the uniform distribution. So, one generally add some more constraints into the optimization problem to get a meaningful class of model distribution

to be used to fit the empirical data. As a simple example, if we maximize the entropy of a random variable having support whole of the real line with the constraints of having known mean and variance, we get the famous Gaussian (normal) distribution.

In the contexts of socio-economic applications, the constraints to derive the maximum entropy distribution is often taken in terms of a known expected utility: $E(u) = \text{constant}$, for a given utility function u . The popular choice of this utility having enough economic justification is the logarithmic entropy

$$u(r) = \log(r). \quad (4)$$

For the RO distributions, if we maximize the the Shannon entropy in (3) subject to the expected utility constraint with the utility given in (4), i.e. $E(\log(r)) = \text{constant}$, along with the normalizing constraint (2), the resulting Max-Ent distribution turns out to the Pareto law.

Note that the utility used in the case of the Pareto distribution only restricts the end of lower ranks by the consideration of the $\log(r)$ terms. Motivated by the failure in modeling the other end of ranks, we propose to add one more constraint in terms of the terms $\log(N + 1 - r)$. This leads to a bivariate utility function, under the rank-size context, of the form

$$u(r) = \left(\begin{array}{c} \log(r) \\ \log(N + 1 - r) \end{array} \right). \quad (5)$$

It is to be noted that the choice of this particular utility function puts equal weightage to both ends of the ranks keeping intact the interpretations and the justifications of logarithmic utility in socio-economic contexts. We can then can consider the expected utility constraints in terms of the newly proposed bivariate utility function as

$$E(\log(r)) = \sum_{r=1}^N \log(r) f(r) = c_1, \quad (6)$$

$$E(\log(N + 1 - r)) = \sum_{r=1}^N \log(N + 1 - r) f(r) = c_2, \quad (7)$$

for two constants c_1 and c_2 , and maximize the Shannon entropy in (3) under these conditions along with (2). To solve this maximization problem, the method of Lagrange multipliers is used and as such the objective function can be written as

$$H(f_1, \dots, f_N) = - \sum_{r=1}^N f_r \log f_r + \lambda_0 \left(\sum_{r=1}^N f(r) - 1 \right) + \lambda_1 \left(\sum_{r=1}^N \log(r) f_r - c_1 \right) + \lambda_2 \left(\sum_{r=1}^N \log(N + 1 - r) f_r - c_2 \right),$$

where we denote $f_r = f(r)$ for $r = 1, \dots, N$ and $\lambda_0, \lambda_1, \lambda_2$ are the necessary Lagrange multipliers. Taking derivatives with respect to f_r lead to the equations

$$- \log f_r - 1 + \lambda_0 + \lambda_1 \log r + \lambda_2 \log(N + 1 - r) = 0, \quad r = 1, \dots, N, \quad (8)$$

and derivatives with respect to $\lambda_0, \lambda_1, \lambda_2$ lead to Equations (2), (6) and (7), respectively. Now, solving (8), we get the Maximum entropy RO distribution f_r^* as given by

$$\begin{aligned} \log f_r^* &= (\lambda_0 - 1) + \log r^{\lambda_1} (N + 1 - r)^{\lambda_2} = 0, \\ f_r^* &= 2^{\lambda_0 + 1} r^{\lambda_1} (N + 1 - r)^{\lambda_2}, \quad r = 1, \dots, N, \end{aligned} \quad (9)$$

which is exactly in the same form as the DGB distribution in (1) with $a = -\lambda_1$, $b = \lambda_2$ and $A = 2^{\lambda_0 + 1}$. Note that λ_0 is to be obtained by normalizing the equations $\sum_{r=1}^N f_r^* = 1$ which makes equivalently A as the normalizing constant. The two other parameters λ_1 and λ_2 , and equivalently (a, b) , depend on the given constant c_1 and c_2 and hence define a class of MaxEnt distributions given by (1). The scaling parameters (a, b) also characterize the shape of the MaxEnt DGB distribution [7]. This analysis provides a natural way to obtain the DGB distribution as a maximum entropy distribution under the expected utility constraints with an extremely intuitive bivariate utility function.

The corresponding value of the maximum Shannon entropy is given by

$$S_{\max}(a, b) = S(f^*) = - \log A - A \sum_{r=1}^N \frac{(N + 1 - R)^b}{r^a} [b \log(N + 1 - r) - a \log r], \quad (10)$$

which provides the maximum amount of uncertainty present in the corresponding RO distribution under the constraints in (6)–(7) and hence depends on c_1 , c_2 or equivalently on the distributional (scaling) parameters (a, b) ; see [7] for its behavior with changing parameter values.

Since the constants c_1 and c_2 in the Max-Ent derivation of the DGB distribution are not known in practice, while using this MaxEnt distribution to model a real-life population, the associated parameters (a, b) need to be based on the empirical data. We have used a simple, yet most efficient, method of estimation via the maximum likelihood approach and subsequent model checking via the Kolmogorov-Smirnov (KS) error metric between the observed and the fitted (cumulative) probabilities; these methods are described briefly in Appendix A. Based on the estimated values (\hat{a}, \hat{b}) of the parameters (a, b) , we can then also estimate the maximum uncertainty present in the empirical distribution as $\hat{S}_{\max} = S_{\max}(\hat{a}, \hat{b})$. The estimated maximum entropy value \hat{S}_{\max} would help us to characterize the underlying socio-economic variable along with their distributional shape analyses via (\hat{a}, \hat{b}) .

III. APPLICATIONS IN MODELING SOCIO-ECONOMIC FACTORS WITHIN A SINGLE COUNTRY

In this section, we present the results obtained by the applications of the Maximum Entropy Rank-Order distribution for a few socio-economic variables within a single country. With the motivation to validate our result with different types of data which are diverse in character, we have chosen city size, income data and election results for different time windows according to the availability of public data. The results of the goodness-of-fit test highly signify the importance of the proposed rank-order distribution for all such cases. Moreover, the entropy analysis explains the uncertainty in their distributions over the years in all cases.

A. City Size distribution for Japan

Despite being just the 61st largest country in the world by area, Japan is one of the most populous countries in the world. The last set of official figures [20] pertaining to Japan's population were released at the time of the 2015 census and the final statistics showed there were 127,094,745 people, which would make Japan the 11th largest country in the world. However, the most recent estimate places the number lower at 126.71 million, still the world's 10th most populous country. Though in decline, it still holds that position in 2019 with an estimated 126.85 million people. The data show the population is shrinking in 39 areas of the country, and growing in eight. Japan's nine major urban areas account for 53.9 % of the total population, with Greater Tokyo now home to 28.4%. Rural areas, on the other hand, are being hit by severe declines. The official census of Japan is performed in every five years, 2015 being the latest. According to latest estimate [20], its largest city, Tokyo, has over 8 million residents while there are additional 13 cities with population over 1 Million. Besides, 191 cities have population in the range of 100,000 to 1 Million and 540 cities with number of people within the range of 10,000 to 100,000. Here, we consider the census data of the population of Japanese cities with at least 20000 inhabitants for the years 1995-2010.

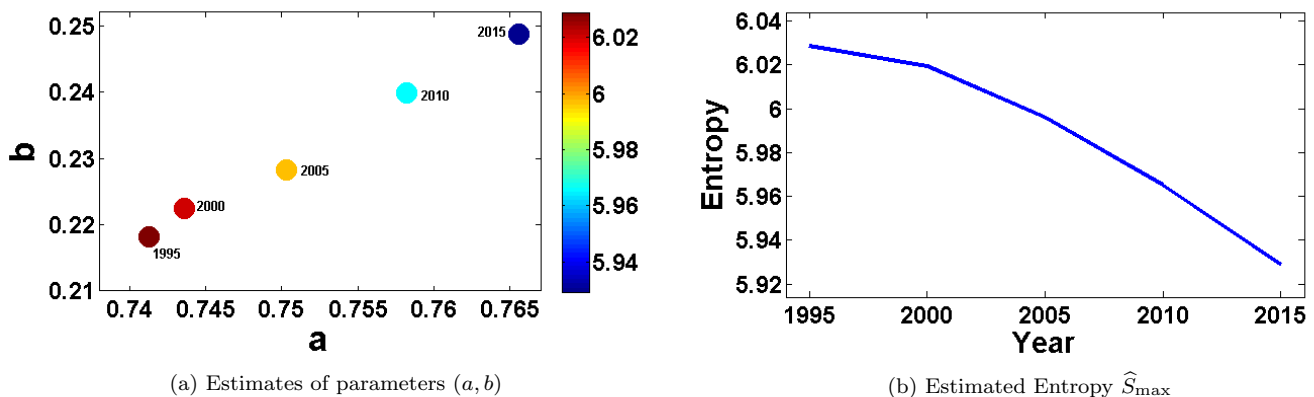


FIG. 1: Estimates of the parameters (a, b) and the maximum entropy values (\hat{S}_{\max}) for the MaxEnt RO distribution fitted to the Japan's city-size data over different years

We have fitted the MaxEnt RO distribution, i.e. the DGB distribution, for the empirical data of Japan's city-sizes for each census years. For brevity, detailed results are presented in Supplementary Table I and Figure 8, which show the excellent fits for our DGD distribution for each years with the KS error measure being only 0.0133 – 0.0149. To illustrate the power of the proposed MaxEnt approach for further in-depth analyses, we present the estimates of the scaling parameters (a, b) and the maximum entropy value \hat{S}_{\max} in Figure 1. One can clearly observe that the entropy of the Japan's city-size distribution is decreasing sharply over the years; it signifies that the larger cities are becoming even larger and smaller cities are becoming even smaller in general. Further, there is a consistent change in the shape of the fitted RO distribution with increasing values of both the scaling parameters (a, b). These provide a mathematical explanation, along with the underlying mechanism, of the fact that more people are continuously moving from rural areas or small towns in Japan to the larger cities over the past twenty years. Urban city dynamics of Japan is thus becoming vulnerably extreme and needs urgent planning for their sustainability.

B. Income distributions of USA: Personal vs. Household Incomes

As our second illustration, we consider grouped data on the personal and the household income in USA for the years 2012 to 2017. These data are collected from the Current Population Survey (CPS), an annual social and economic supplement, sponsored jointly by the U.S. Census Bureau and the U.S. Bureau of Labor Statistics (BLS). The available grouped data [21, 22] provide the number of people (in thousands) or households in 41 different income groups; the personal income refers to people of ages 15 years and above but the household income data covers *all* households in USA. From the years 2012 only, the income classes are given in the interval of \$2499 and \$4999, respectively, for the personal and household income data; the respective last groups correspond to the persons having income \geq \$100000 and the households having income is \geq \$ 200000 per /year.

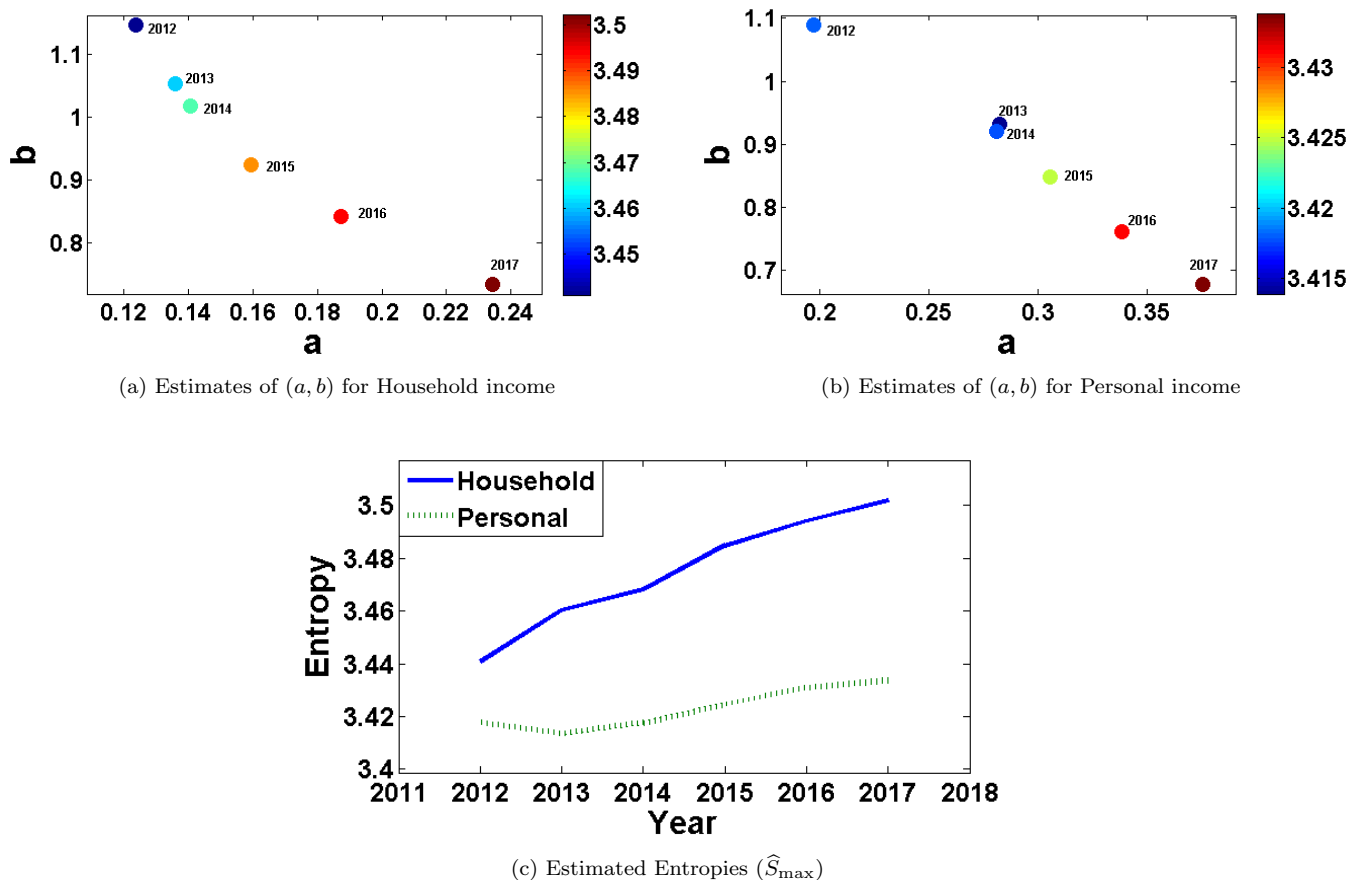


FIG. 2: Estimates of the parameters (a, b) and the maximum entropy values \hat{S}_{\max} for the MaxEnt RO distribution fitted to the personal and household income data of USA over different years

We employ our MaxEnt approach to fit the DGB distribution to these data which again yields remarkably good fits having KS error in the range [0.0149, 0.0255] only; the detailed results are given in Supplementary Tables II-III and Supplementary Figures 0-10, and the parameter estimates along with \hat{S}_{\max} are plotted in Figure 2 for both personal and household income data. Note that, for both the personal and household income, the scaling parameters follow a prominent changing pattern over the years — values of b are in a similar range in both cases and decrease over time, whereas the value of a is increasing over the years and are higher for personal income data. Further, in contrast to Japan’s city-size distribution, the entropies \hat{S}_{\max} of the fitted MaxEnt distribution to both the personal and household incomes of USA are seen to have an increasing trend over the years. These indicate that the difference in the number of people/households in different income groups are decreasing in general.

The entropy and its increment rate are much greater for the household incomes compared to the personal incomes. Thus, the household income distributions in USA are relatively closer to the uniform distribution than personal incomes in each year and further moving towards more uniformity over the time. Does it signify that the income inequality among households in USA are decreasing over time? Although it needs further focused investigations considering household sizes, there is definite hope since the entropy in 2017 is not very far from the global maximum value (corresponding to uniform distribution) of $\log(N) = 3.714$. For personal income, however, the rate of increment is significantly slower over the last five years and might look to stabilize in more recent years; the income inequality among people of USA is still looking far from being close to uniformity.

C. Indian Lok Sabha Election Results

Not all socio-economic factors behave so nicely as in the previous two examples if they are not governed by a well-structured economy and hence also depends on the corresponding country. To illustrate the applicability of our proposed MaxEnt RO approach beyond such cases as well, our third illustration here is to focus on a completely different type of data on the winners of Indian Lok Sabha elections. India is a federation with a parliamentary system governed under the Constitution of India, where the Parliament consists of the President of India and the two Houses of Parliament known as the Council of States (Rajya Sabha) and the House of the People (Lok Sabha). Members of the Lok Sabha are elected by adult universal suffrage and a first-past-the-post system to represent their respective constituencies; more lucidly, they are elected by being voted upon by all adult citizens of India, from a set of candidates who stand in their respective constituencies. Every adult citizen of India can vote only one candidate and only in their own constituency, and the candidate with the highest number of votes is elected. Although the maximum strength of the House allotted by the Constitution of India is 552, currently it has 545 members including 543 (at max) elected members and 2 (at max) nominated members of the Anglo-Indian Community by the President of India. The Lok Sabha (House of the People) was duly constituted for the first time on 17 April 1952 after the first General Elections held from 25 October 1951 to 21 February 1952. Subsequently, following the same procedure and as the situation arose, later the election was conducted 17 times till date most of which are in a five year interval (except few situations of political crisis). Due to the complex nature of the process, it is a definite challenge to mathematically model and analyze the voting pattern in different Lok Sabha elections and their evolution over time. Here, for the first time, we model the winner’s vote percentage and the percentage of vote-margin of the winning candidate from the second-placed candidate for a Lok Sabha election in India by the proposed MaxEnt approach with the DGB distribution. As per the availability of the data [23], we consider the 11 Lok Sabha elections from the year 1980 to 2019.

It is really interesting to see the effectiveness of the MaxEnt DGB distribution to produce excellent fits for such a complex phenomena as well with extremely low KS error in the range 0.0019 to 0.0084 only; see Supplementary Tables IV–V for detailed results and Supplementary Figures 11–12 for the actual fits. The parameter estimates and the maximum entropy values are plotted in Figure 3. Although there is no clear pattern of the distributional shapes (i.e., estimated values of a and b) over the years, their entropy (\hat{S}_{\max}) follow a clearly similar trend. However, the entropies of the winner’s vote percentage are seen to be significantly higher than those of the vote-margin percentage; the values of \hat{S}_{\max} in the first case is almost the same as the corresponding global maximum ($\log(N)$) so that the winner’s vote percentage is mostly uniform in every Indian Lok Sabha election. Further, for both the cases, \hat{S}_{\max} has a significant increment (structural break) from the year 2004 to 2009, after remaining mostly stable before 2004. Other than a significant increase in the number of constituencies (N), there might also be some socio-political reasons to explain such a drastic change in voting pattern which will be an interesting future question to investigate.

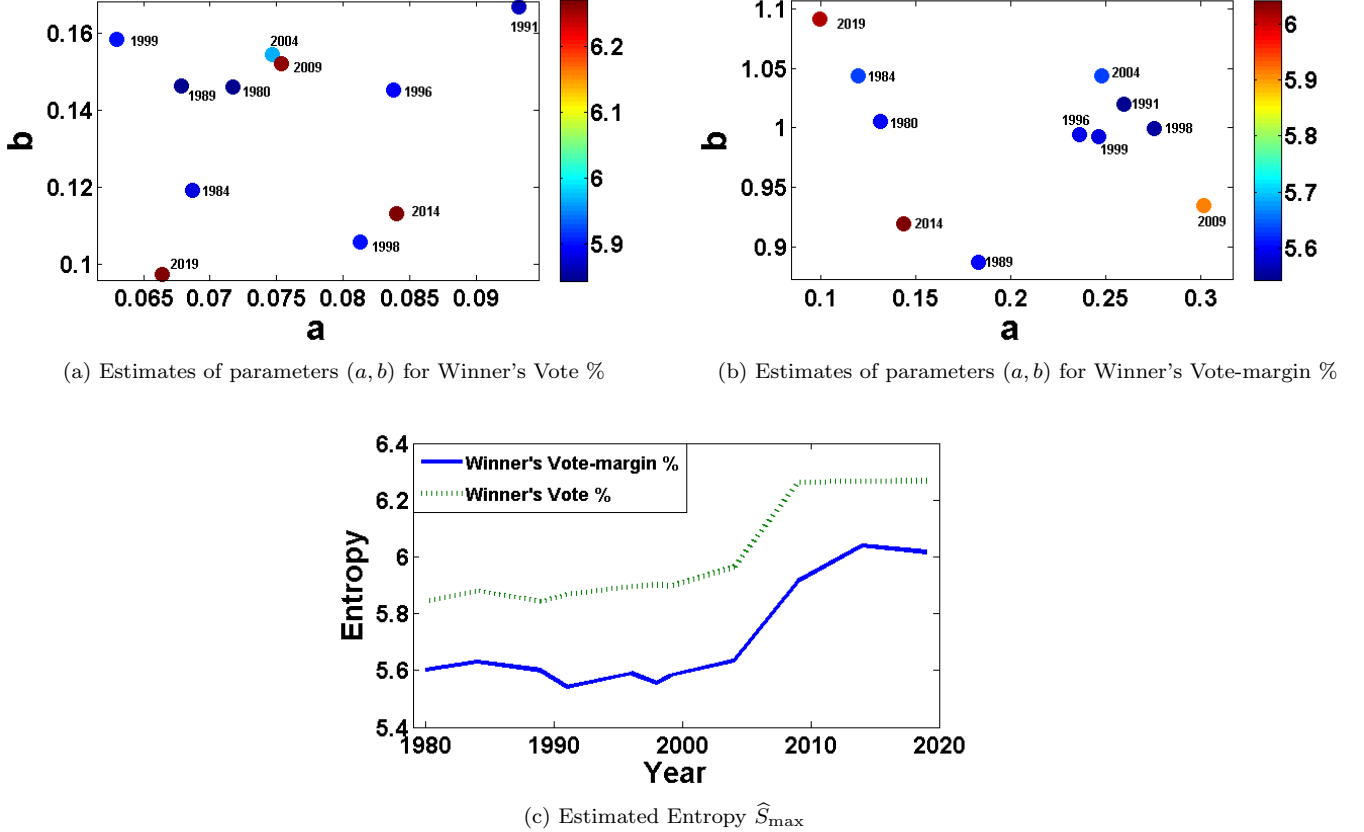


FIG. 3: Estimates of the parameters (a, b) and the maximum entropy values \hat{S}_{\max} for the MaxEnt RO distribution fitted to the data on Winner's vote percentage and Vote-margin percentage in Indian Lok Sabha elections in different years

IV. APPLICATIONS IN GLOBAL MODELING ACROSS DIFFERENT COUNTRIES

In this section, we will illustrate the universality of the MaxEnt RO distribution even for global modeling of various socio-economic indicators across different countries. In particular, we have considered the data for population, percentages of available agricultural land, per capita GDP and the ratio of market capitalization to GDP (known as the *Buffet indicator*) from different countries across the world; the time frames of the analyses and the countries considered are according to the availability of publicly available data in each case.

A. Distribution of Population for different countries

As the first illustration of our global modelling, we have studied the distribution of the country sizes in terms of their population for each year from 2001 to 2018 obtained from [24]; these cover around 190 major countries and/or territories across the world. The excellent fit of the MaxEnt RO distribution for this case can again be noted from Supplementary Table VII and Figure 13; the KS error ranges from 0.0558 to 0.0588 only. The parameter estimates are plotted in Figure 4 along with the corresponding entropy. It is interesting that the countries around the world have a similar distributional structure as that of the cities within a country and we should be able to explain them as well with a city size law; see also [7]. However, unlike Japan's city-size distribution, the entropy of the country-size distribution is increasing over time indicating the decreasing discrimination between the population in different countries. The change is, although, significantly slower with values ranging from 3.5678 to 3.6516 only over the last 18 years and still significantly away from the uniformity (corresponding global maximum of entropy is $\log(N) = 5.247$). The shape of the distribution is also changing gradually in a fixed pattern with decreasing a and increasing b . Additionally, the changes in countries' population distribution are observed to be significant around the years 2003 and 2011, which would be an interesting topic for further investigation.

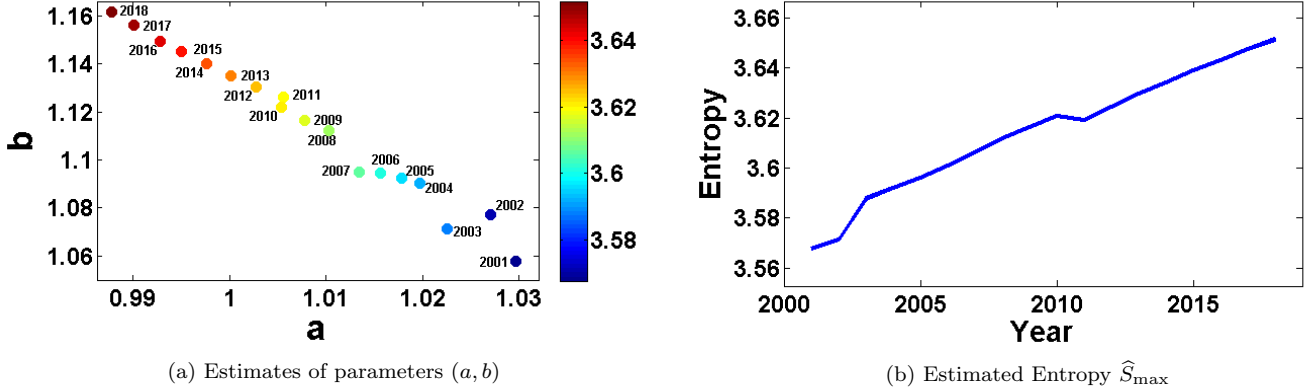


FIG. 4: Estimates of the parameters (a, b) and the maximum entropy values \hat{S}_{\max} for the MaxEnt RO distribution fitted to the countries' population data over different years

B. Distribution of Agricultural land across countries

We now discuss a fascinating socio-economic indicator, probably not studied previously, namely the percentage of available agricultural land in different countries across the world. This study may help the Policymakers to create a better and more coherent policy environment to meet food demand sustainably. Agricultural land, defined by the Food and Agriculture Organization (FAO), refers to the share of land area that is arable, under permanent crops, and under permanent pastures. We have considered the data from [25], collected annually by FAO, over a time window of 14 years (2003 – 2016) for around 192-194 countries as per the availability.

Once again we apply the proposed MaxEnt approach with the DGB distribution which is seen to fit the empirical data exceptionally well with a very small KS error of 0.0044 – 0.0074; see Supplementary Table VIII and Figure 14 for detailed results and model fits for each year. Remarkably here, the entropy value \hat{S}_{\max} remains mostly stable over the years (except for sudden increase around the year 2006-07); it varies over 5.05 – 5.09 only. However, the distributional shapes, studied through the estimated values of (a, b) in Figure 5, are different in most years and form two prominent clusters before and after the years 2007. It would be interesting to investigate such a distributional change in world's agricultural land percentage from 2007! We may point out here that worldwide food prices increased dramatically in 2007 and the first and second quarter of 2008 [28], creating a global crisis and causing political and economic instability and social unrest in both poor and developed nations.

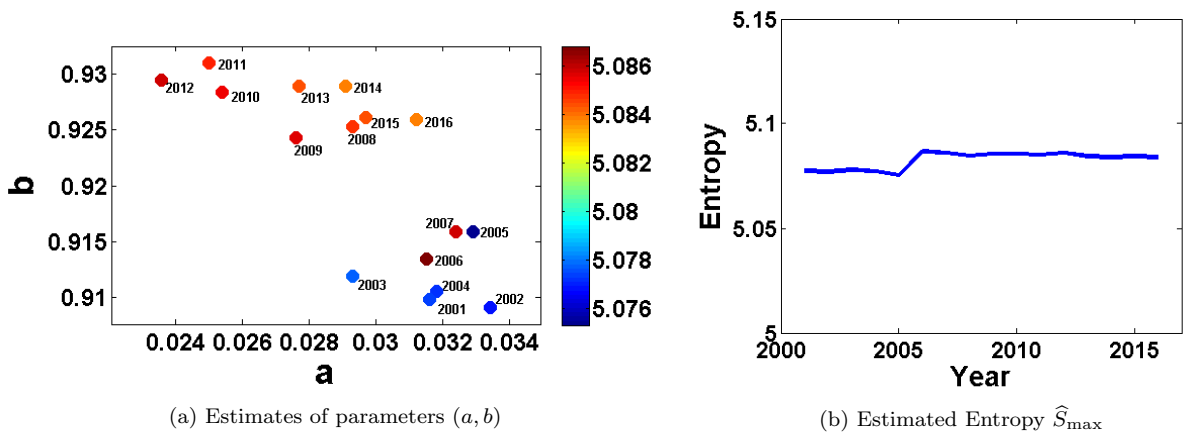


FIG. 5: Estimates of the parameters (a, b) and the maximum entropy values \hat{S}_{\max} for the MaxEnt RO distribution fitted to the Agricultural land percentage data over different years

C. Per capita GDP for various countries over different years

Another very important global socio-economic indicator is the Gross domestic product (GDP), a national accounts indicator of a country's economic performance and strength. It is measured by the added value of all final goods and services produced in a country during a specific time period or by adding every persons income during that time period. Per capita GDP is also used to describe the standard of living of a population, with a higher GDP meaning a higher standard of living. Here, we have used the publicly available data on the per capita GDP of about 100 countries for the years 2001–2018, according to their availability from [26], and applied the proposed MaxEnt approach. As can be seen from the detailed results given in Supplementary Table IX and Figure 15, the DGB distribution again yields very good fit for the per capita GDP data across the world in each year – the KS ranges in [0.0136–0.0293] only.

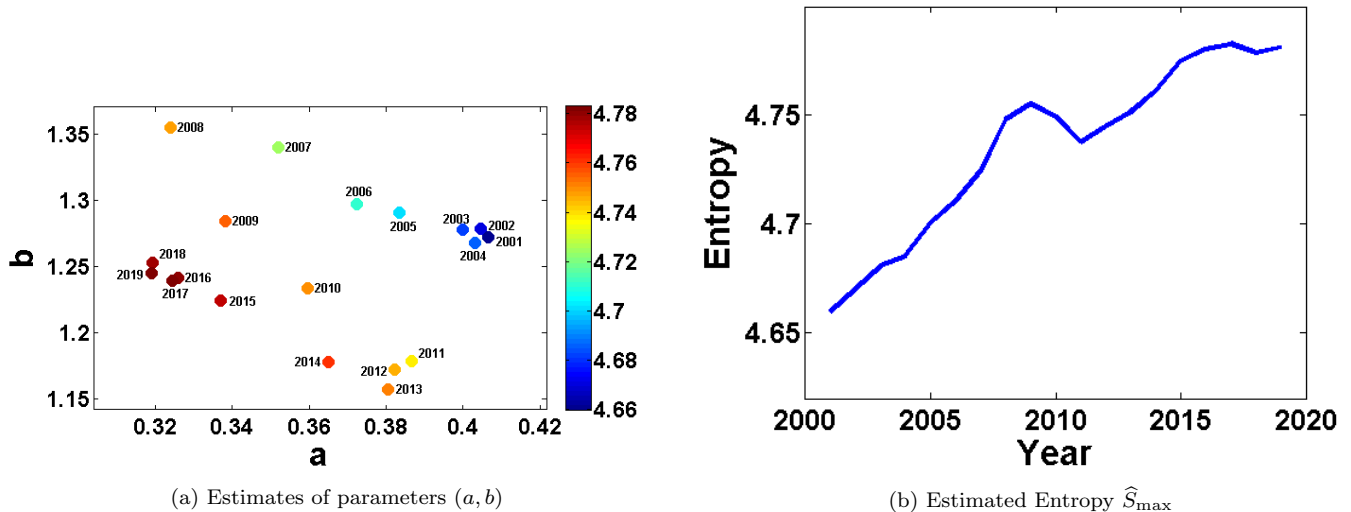


FIG. 6: Estimates of the parameters (a, b) and the maximum entropy values \hat{S}_{\max} for the MaxEnt RO distribution fitted to the per capita GDP data over different years

From the plots of the estimated parameters (a, b) and the corresponding maximum entropy \hat{S}_{\max} in Figure 6, a clear trend of the entropy is visible over the years although no pattern emerges for distributional shapes. On the whole, from the years 2001 to 2018, world's per capita GDP (country-wise) seems to have an increasing trend of the underlying entropy measure indicating the decreasing inequality among countries' economic strengths. However, an interesting phenomenon is also observed around the year 2010 when the entropy abnormally break the pattern to decrease from 2009 to 2011. Without a detailed analysis, we are not in a position to remark whether this result is due to the 2007-2010 US financial crisis.

D. Buffet Indicators of different countries across the world

Our last illustration is to emphasize that the proposed MaxEnt approach is not necessarily limited to count, continuous or percentage data only; rather it can also be used to successfully model the ratio-type socio-economic indicators as well. Here, for example, we consider the Buffet indicators of different countries that describe the ratio of Market Capitalization and % of GDP. This financial market indicator signifies the percentage of GDP that represents stock market value and used to determine whether an overall market is undervalued or overvalued compared to a historical average. This is probably the best single measure of where valuations stand at any given moment. It is a measure of the total value of all publicly traded stocks in a market divided by that economy's gross domestic product (GDP). The ratio compares the value of all stocks at an aggregate level to the value of the country's total output.

Here, we have used the data for around 190 countries from the year 2006 to 2016, as available in [27]. Results of the MaxEnt analyses of these data are given in Supplementary Table VI and Figure 16; the KS values ranges in [0.0385, 0.0621] indicating yet another example of excellent DGB fit. However, unlike the previous cases, there is no prominent pattern in the fitted RO distributions to the Buffet indicators over different years both in terms of parameter estimates and the entropy values; see Figure 7. We should note here a potential issue with the Buffett

Indicator; the underlying assumption of stable corporate earnings relative to economic activity may be wrong, or it may be correct for the United States but not for other markets. More investigation is required for further in-depth analyses.

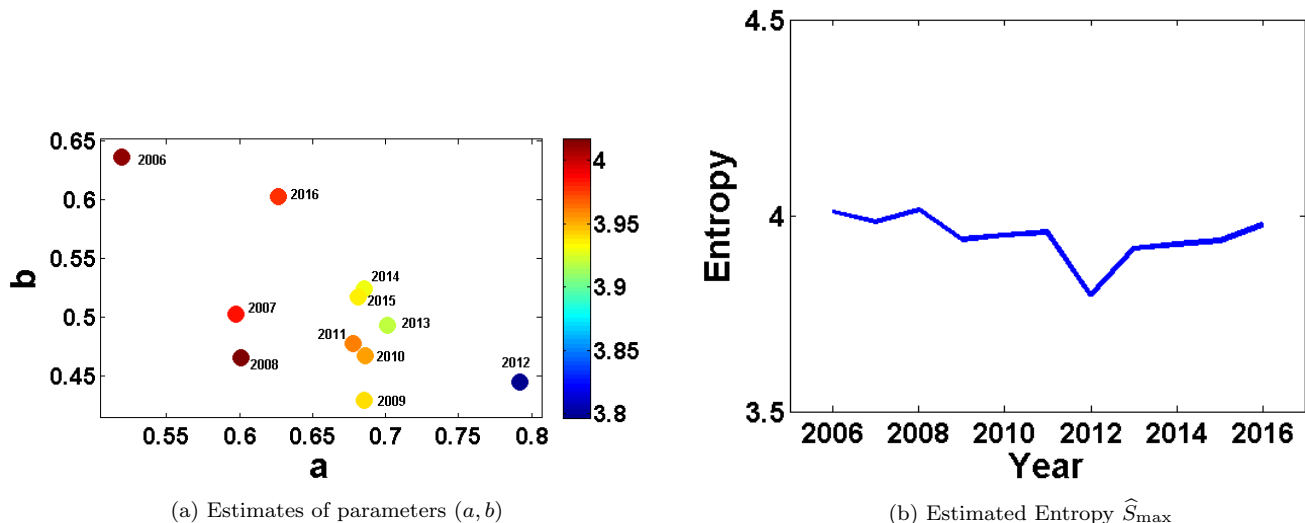


FIG. 7: Estimates of the parameters (a, b) and the maximum entropy values \hat{S}_{\max} for the MaxEnt RO distribution fitted to the data of Buffet Indicators of various countries over different years

V. DISCUSSIONS

Recently, there was a proposal showing a universal behavior defined in terms of a functional relation for rank ordered distributions that holds accurately along the whole rank range for an impressive amount of phenomena of very diverse nature [6]. This distribution goes beyond power laws since it is a two parameter relation that reduces to a power law when one of them is zero. It is observed that this distribution is very much useful in modelling many socio-economic factors providing excellent fits when validated with real world empirical data. However, the underlying theory responsible for the success of this particular RO distribution is not explored properly. This paper is the first to provide a derivation of this particularly useful RO distribution as a natural *maximum entropy distribution* under the appropriate bivariate utility constraints. Moreover, here we have also illustrated its acceptability in universal modeling of different types of socio-economic factors. In particular, we have considered data for diverse socio-economic factors within a country as well as across the countries to demonstrate our theory. In this maximum entropy framework, the two parameters corresponding to the distribution of various socio-economic indicators can be thought of as two *sensors* or *latentdrivers* of the respective dynamics and may further be associated with observable economic, social or environmental factors. The estimated values of distributional parameters, *sensors*, along with the *entropy* helped us to investigate the underlying theory of the distribution. The evolution of the *entropy* over a time span showed how the underlying uncertainty in the distribution changes over time. It is very fascinating to note that the world food crisis in 2007 has an inherent imprint over the percentage of agricultural land data analysis (See Fig. 5). Similarly, the entropy analysis of GDP per capita and Buffet indicator of various countries over many years (Fig. 6 and 7) give hints of the world financial crisis during 2007-2010. We believe that the universal rank-order modeling, along with the underlying entropy analysis for diverse socio-economic measures around the world will shed light on setting policies promoting inclusive, equitable and sustainable development.

Acknowledgment:

PS acknowledges Indian Statistical Institute, Kolkata, India for allowing her to work as a summer/project trainee in the Physics and Applied Mathematics Unit.

Appendix A: Method: Fitting the Max-Ent RO distribution to Empirical Data

Suppose there are N items (data-points) whose ranks and sizes are, respectively, denoted as r_i and x_i for $i = 1, \dots, N$. We need to find a best fitted DGB distribution through the estimation of the parameters (a, b) from the empirical data. We use the maximum likelihood approach to estimate (a, b) by maximizing the likelihood function

$$L(a, b) = \prod_{i=1}^N f_{(a,b)}(r_i)^{x_i} = \prod_{i=1}^N \frac{(N+1-r_i)^{bx_i}}{r_i^{ax_i}} A^{x_i}, \quad (\text{A1})$$

or, equivalently the log-likelihood function $\ell(a, b) = \log L(a, b)$. Our numerical illustrations are performed in the software MATLAB (version14a) using the in-built function 'fminsearch'; see [7] for more details and justifications.

After estimating the parameters as (\hat{a}, \hat{b}) , we compute the predicted size of r_i as $p_i = \left(\sum_{i=1}^N x_i \right) f_{(\hat{a}, \hat{b})}(r_i)$, and compare it with the observed sizes x_i to investigate the goodness-of-fit of our RO model. The overall error in this fit is quantified through the Kolmogorov-Smirnov (KS) measure between the predicted and the observed cumulative frequencies of ranks:

$$KS = \max_{1 \leq i \leq N} \left| \left(\sum_{j:r_j \leq r_i} p_j \right) - \left(\sum_{j:r_j \leq r_i} x_j \right) \right|. \quad (\text{A2})$$

- [1] David Hume, A Treatise of Human Nature, (1738)
- [2] Auguste Comte, The Positive Philosophy, Vols. 1, 2, and 3, trans. and cond. H. Martineau (London: George Bell & Sons, 1896)
- [3] 1835. Sur l'homme et le dveloppement de ses facults, ou Essai de physique sociale. 2 volumes, (1835), 1842. A Treatise on Man and the Development of His Faculties (1842)
- [4] E. T Jaynes, Physical Review **106** (4) , 620 (1957)
- [5] J.N. Kapur, Maximum-entropy models in science and engineering. John Wiley & Sons (1989).
- [6] G. Martnez-Mekler, R.A. Martnez, M.B. del Ro, R. Mansilla, P. Miramontes, and G. Cocho, PLoS One, **4(3)** (2009) e4791.
- [7] A. Ghosh and B. Basu, Physica A: Statistica Mechanica and its Applications, 528, 121094 (2019)
- [8] M. Ausloos, and R. Cerqueti, PloS one, **11(11)** (2016) e0166011.
- [9] R. Alvarez-Martinez, G. Martinez-Mekler, and G. Cocho, Physica A: Statistical Mechanics and its Applications, **390** (1) (2011) 120
- [10] R. Alvarez-Martinez, G. Cocho, R.F. Rodriguez, and G. Martnez-Mekler, Physica A: Statistical Mechanics and its Applications, **402**, (2014), 198
- [11] O. Fontanelli, P. Miramontes, G. Cocho and W. Li, Royal Soc. Open Science, **4** 170281 (2017)
- [12] R. Alvarez-Martinez, G. Cocho and G. Martinez-Mekler, Chaos: An Interdisciplinary Journal of Nonlinear Science, **28(7)** (2018) 075515.
- [13] X. Wu, Journal of Econometrics **115**, pp. 347-354 (2003)
- [14] K. Gangopadhyay and B. Basu, Physica A **388** (2009) 2682
- [15] A. Ghosh, K. Gangopadhyay and B. Basu, Physica A **390** (2011) 83
- [16] K. Bury K. Statistical Distributions in Engineering. Cambridge, UK: Cambridge University Press; 1999. p. 362.
- [17] JB McDonald, Some Generalized Functions for the Size Distribution of Income. Econometrica. 1984;52:647664
- [18] Silviu Guiasu and Abe Shenitzer, The Mathematical Intelligence, **7**, NO. 1, 42 (1985) Springer-Verlag New York
- [19] S.Press, K. Ghosh, J. Lee, and Ken A. Dill, Rev. Mod. Phys. **85**, 1115 (2013)
- [20] <https://www.citypopulation.de/Japan.html>
- [21] <https://www.census.gov/data/tables/time-series/demo/income-poverty/cps-pinc/pinc-01.html>
- [22] <https://www.census.gov/data/tables/time-series/demo/income-poverty/cps-hinc/hinc-01.html>
- [23] <https://www.electionsinindia.com/india/parliament-lok-sabha-constituency-elections>
- [24] <https://www.imf.org/external/datamapper/LP@WEO/TWN/KOR/JPN>
- [25] <https://data.worldbank.org>
- [26] <https://www.imf.org/external/datamapper/PPPPC@WEO/OEMDC/ADVEC/WEOWORLD>
- [27] <https://www.ceicdata.com/en/indicator/market-capitalization-nominal-gdp>
- [28] World Food Situation, FAO. Archived from the original on 29 April 2011. Retrieved 24 April 2011.

Appendix B: Supplementary Tables

TABLE I: Estimated measures for Japanese Cities (human settlements) along with total number of cities (N) and the sizes x_{\min}, x_{\max} of the smallest and the largest cities, respectively.

Year	Summary			RO Fit			Entropy
	N	x_{\min}	x_{\max}	\hat{a}	\hat{b}	KS	S
2015	976	16742	9272740	0.7656	0.2487	0.0149	5.9292
2010	985	16628	8945695	0.7582	0.2399	0.0140	5.9653
2005	985	18060	8489653	0.7503	0.2283	0.0136	5.9962
2000	985	16504	8134688	0.7436	0.2225	0.0133	6.0197
1995	985	15171	7967614	0.7413	0.2182	0.0134	6.0289

TABLE II: Parameter estimates for the distribution of Personal Income for USA, along with total number of income groups (N) and the sizes x_{\min}, x_{\max} of the smallest and largest income groups respectively.

Year	summary			RO Fit			Entropy
	N	x_{\min}	x_{\max}	\hat{a}	\hat{b}	KS	S
2017	41	0780.0000	24926.0	0.3751	0.6772	0.0149	3.4338
2016	41	0770.1000	22426.1	0.3381	0.7619	0.1640	3.4310
2015	41	0712.0000	20755.0	0.3053	0.8480	0.0179	3.4250
2014	41	0683.0000	19063.0	0.2811	0.9209	0.0189	3.4178
2013	41	0672.0000	19108.0	0.2825	0.9310	0.0184	3.4138
2012	41	0575.8441	15727.4	0.1975	1.0897	0.0237	3.4179

TABLE III: Parameter estimates for the distribution of Household Income for USA, along with total number of income groups (N) and the sizes x_{\min}, x_{\max} of the smallest and the largest cities, respectively.

Year	Summary			RO Fit			Entropy
	N	x_{\min}	x_{\max}	\hat{a}	\hat{b}	KS	S
2017	41	588	9874	0.2344	0.7325	0.0188	3.5021
2016	41	482	8775	0.1874	0.8418	0.0193	3.4944
2015	41	431	7640	0.1595	0.9233	0.0188	3.4851
2014	41	436	7005	0.1404	1.0173	0.0243	3.4683
2013	41	347	7085	0.1358	1.0536	0.0255	3.4606
2012	41	364	7157	0.1235	1.1478	0.0243	3.4411

TABLE IV: Parameter estimates for the distribution of vote percentage share of winner candidate in terms of percentage for India... in their respective constituency along with total number of Parliamentary constituencies (N) and the sizes x_{\min}, x_{\max} of the smallest and largest percentage of winners' vote percentage respectively.

Year	Summary			RO Fit			Entropy
	N	x_{\min}	x_{\max}	\hat{a}	\hat{b}	KS	S
2019	534	32.40%	74.47%	0.0664	0.0975	0.0021	6.2701
2014	535	27.30%	75.79%	0.0840	0.1132	0.0035	6.2673
2009	535	14.19%	78.80%	0.0754	0.1521	0.0019	6.2631
2004	398	25.98%	77.16%	0.0747	0.1544	0.0036	5.9672
1999	371	20.83%	74.91%	0.0630	0.1583	0.0027	5.8984
1998	371	25.55%	86.70%	0.0813	0.1058	0.0028	5.9028
1996	371	24.36%	78.47%	0.0838	0.1452	0.0037	5.8967
1991	363	23.06%	90.12%	0.0932	0.1667	0.0030	5.8697
1989	351	27.15%	84.08%	0.0678	0.1463	0.0024	5.8440
1984	363	25.81%	83.67%	0.0687	0.1192	0.0027	5.8812
1980	351	22.68%	77.53%	0.0717	0.1460	0.0032	5.8434

TABLE V: Parameter estimates for the distribution of vote percentage share margin of the winner candidate in terms of percentage for India in their respective constituency along with total number of Parliamentary Constituencies (N) and the sizes x_{\min}, x_{\max} of the smallest and largest percentage of winners' vote margin percentage respectively.

Year	Summary			RO Fit			Entropy
	N	x_{\min}	x_{\max}	\hat{a}	\hat{b}	KS	S
2019	534	0.02%	52.73%	0.0993	1.0916	0.0029	6.0176
2014	535	0.07%	56.25%	0.1435	0.9190	0.0056	6.0422
2009	535	0.04%	70.10%	0.3019	0.9349	0.0055	5.9162
2004	398	0.06%	61.41%	0.2480	1.0443	0.0054	5.6363
1999	371	0.13%	53.54%	0.2465	0.9926	0.0031	5.5839
1998	371	0.01%	73.41%	0.2758	0.9999	0.0055	5.5568
1996	371	0.06%	72.00%	0.2363	0.9947	0.1170	5.5914
1991	363	0.03%	87.19%	0.2595	1.0202	0.0072	5.5429
1989	349	0.16%	70.30%	0.1828	0.8870	0.0034	5.6016
1984	362	0.02%	72.18%	0.1195	1.0437	0.0084	5.6315
1980	351	0.02%	68.49%	0.1316	1.0053	0.0036	5.6045

TABLE VI: Parameter Estimates for Buffet indicator, along with number of countries (N) and the entries x_{\min}, x_{\max}

Year	Summary			RO Fit			Entropy
	N	x_{\min}	x_{\max}	\hat{a}	\hat{b}	KS	S
2016	93	0.083	0981.639	0.6267	0.6023	0.0535	3.9772
2015	93	0.092	1018.500	0.6812	0.5170	0.0494	3.9373
2014	93	0.086	1101.432	0.6854	0.5236	0.0581	3.9282
2013	93	0.084	1118.119	0.7014	0.4933	0.0592	3.9179
2012	93	0.101	1073.692	0.7918	0.4443	0.0467	3.7964
2011	93	0.101	0902.212	0.6776	0.4778	0.0564	3.9596
2010	93	0.066	1178.962	0.6861	0.4672	0.0621	3.9519
2009	90	0.066	1070.925	0.6857	0.4292	0.0569	3.9406
2008	88	0.059	0600.508	0.6012	0.4656	0.0366	4.0175
2007	86	0.069	1244.064	0.5975	0.5024	0.0545	3.9857
2006	85	0.079	0881.286	0.5195	0.6360	0.0385	4.0118

TABLE VII: Estimation of parameters for the distribution of population of various countries in the world, along with number of countries (N) and the entries x_{\min}, x_{\max} for the population

Year	Summary			RO Fit			Entropy
	N	$x_{\min}(\text{Mn})$	$x_{\max}(\text{Mn})$	\hat{a}	\hat{b}	KS	S
2018	192	0.011	1396.982	0.9878	1.1614	0.0588	3.65160
2017	192	0.011	1390.080	0.9901	1.1560	0.0587	3.64770
2016	192	0.011	1382.710	0.9928	1.1493	0.0585	3.64330
2015	192	0.011	1374.620	0.9950	1.1452	0.0584	3.63910
2014	192	0.011	1367.820	0.9976	1.1399	0.0582	3.63440
2013	192	0.011	1360.720	1.0001	1.1351	0.0581	3.62970
2012	192	0.010	1354.040	1.0028	1.1303	0.0580	3.62470
2011	192	0.010	1347.350	1.0056	1.1260	0.0579	3.61910
2010	192	0.010	1340.910	1.0054	1.1219	0.0581	3.62090
2009	192	0.010	1334.500	1.0078	1.1166	0.0580	3.61652
2008	192	0.009	1328.020	1.0103	1.1121	0.0579	3.61180
2007	191	0.009	1321.290	1.0134	1.0951	0.0577	3.60620
2006	191	0.009	1314.480	1.0156	1.0944	0.0575	3.60090
2005	191	0.010	1307.560	1.0178	1.0925	0.0573	3.59620
2004	191	0.010	1299.880	1.0197	1.0901	0.0571	3.59210
2003	190	0.009	1292.270	1.0225	1.0713	0.0567	3.58790
2002	189	0.009	1284.530	1.0270	1.0771	0.0562	3.57140
2001	188	0.019	1276.270	1.0296	1.0577	0.0558	3.56780

TABLE VIII: Parameter estimates for the distribution of percentage of agricultural land in various countries across the world, along with number of countries (N) and the entries x_{\min}, x_{\max} maximum and minimum land percentage in that particular year respectively.

Year	Summary			RO Fit			Entropy
	N	x_{\min}	x_{\max}	\hat{a}	\hat{b}	KS	S
2016	194	0.56%	82.56%	0.0312	0.9259	0.0072	5.0838
2015	194	0.56%	82.56%	0.0297	0.9261	0.0072	5.0843
2014	194	0.57%	82.56%	0.0291	0.9289	0.0072	5.0839
2013	194	0.53%	82.64%	0.0277	0.9289	0.0070	5.0844
2012	194	0.47%	81.30%	0.0236	0.9295	0.0072	5.0859
2011	194	0.51%	83.00%	0.0250	0.9310	0.0074	5.0850
2010	194	0.50%	82.46%	0.0254	0.9284	0.0071	5.0855
2009	194	0.52%	84.64%	0.0276	0.9243	0.0067	5.0856
2008	194	0.45%	83.84%	0.0293	0.9253	0.0068	5.0847
2007	194	0.45%	83.13%	0.0324	0.9159	0.0062	5.0859
2006	194	0.47%	83.96%	0.0315	0.9134	0.0053	5.0868
2005	192	0.47%	84.74%	0.0329	0.9159	0.0044	5.0753
2004	192	0.50%	84.73%	0.0318	0.9105	0.0057	5.0571
2003	192	0.52%	85.29%	0.0293	0.9119	0.0062	5.0778
2002	192	0.47%	85.26%	0.0334	0.9091	0.0063	5.0769
2001	192	0.55%	85.49%	0.0316	0.9098	0.0057	5.0774

TABLE IX: Parameter estimates for GDP per capita, along with number of countries (N) and the entries x_{\min}, x_{\max} for the GDP per capita, respectively.

Year	Summary			RO Fit			Entropy
	N	x_{\min}	x_{\max}	\hat{a}	\hat{b}	KS	S
2019	190	726.885	134622.6	0.3190	1.2451	0.0176	4.7813
2018	190	711.896	130475.1	0.3193	1.2527	0.0175	4.7787
2017	191	680.323	127785.4	0.3244	1.2394	0.0172	4.7830
2016	191	652.481	125307.6	0.3260	1.2416	0.0166	4.7807
2015	191	629.558	130319.6	0.3370	1.2244	0.0165	4.7752
2014	191	606.024	136829.7	0.3651	1.1774	0.0142	4.7613
2013	191	600.193	142845.6	0.3806	1.1567	0.0122	4.7515
2012	191	593.842	146981.8	0.3822	1.1721	0.0126	4.7448
2011	191	560.425	145723.8	0.3866	1.1786	0.0149	4.7379
2010	191	530.043	127195.7	0.3595	1.2338	0.0191	4.7494
2009	191	504.838	111399.6	0.3382	1.2844	0.0225	4.7555
2008	191	502.787	104145.4	0.3239	1.3556	0.0244	4.7482
2007	191	479.299	117053.0	0.3520	1.3403	0.0245	4.7243
2006	190	453.592	115071.8	0.3725	1.2970	0.0253	4.7107
2005	190	431.732	104311.6	0.3834	1.2910	0.0272	4.7006
2004	190	420.928	107274.6	0.4031	1.2681	0.0270	4.6856
2003	189	409.659	95604.29	0.4000	1.2778	0.0284	4.6810
2002	188	406.197	94876.81	0.4045	1.2788	0.0295	4.6705
2001	186	413.190	89695.37	0.4066	1.2722	0.0293	4.6598

Appendix C: Supplementary Figures

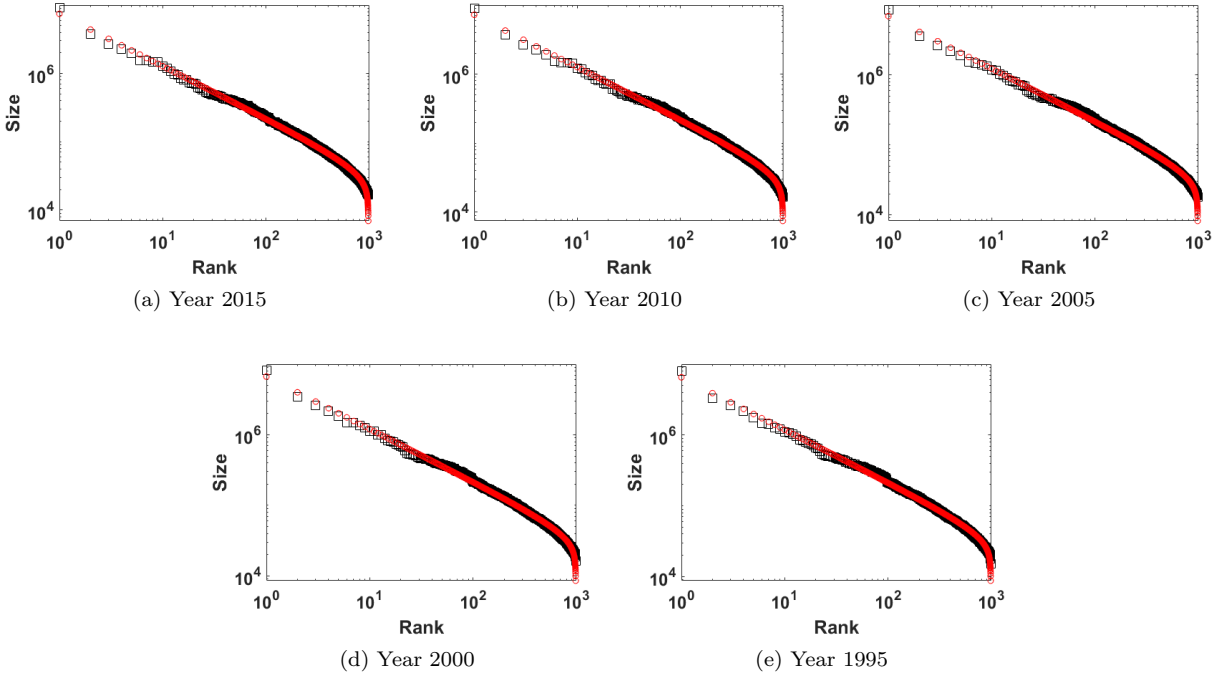


FIG. 8: Plots of actual (Black square) and predicted (Red circle) sizes over the rank for the city size of Japan

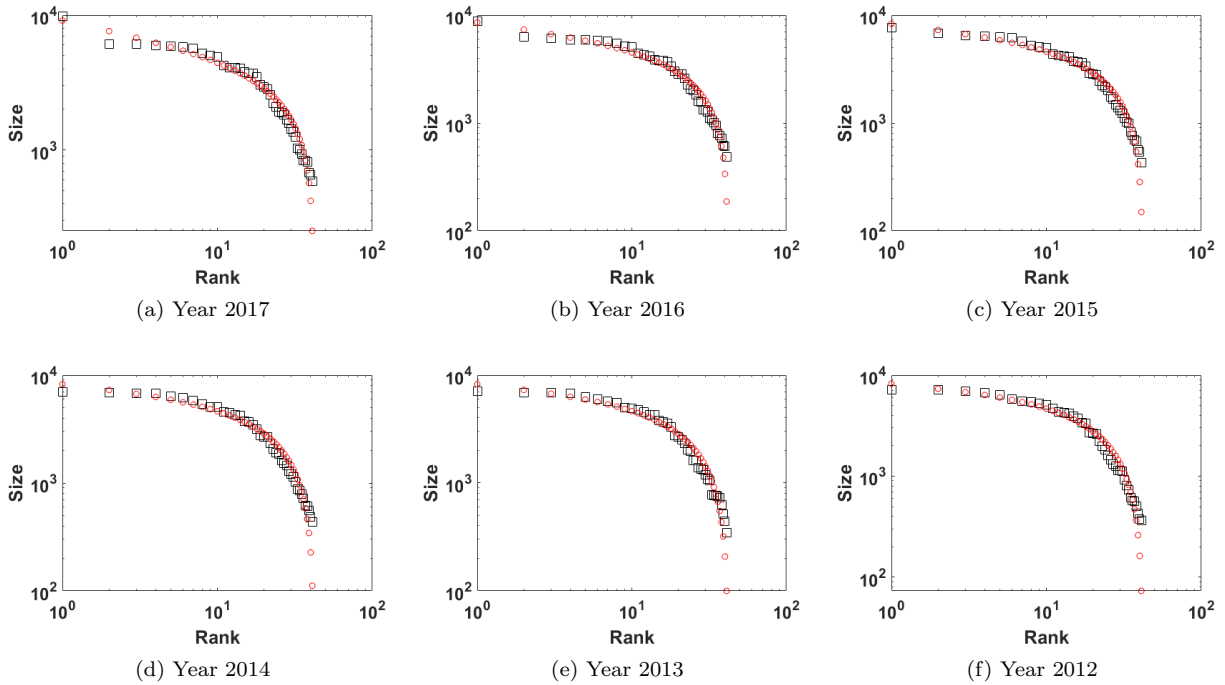


FIG. 9: Plots of actual (Black square) and predicted (Red circle) sizes over the rank for the household income of USA

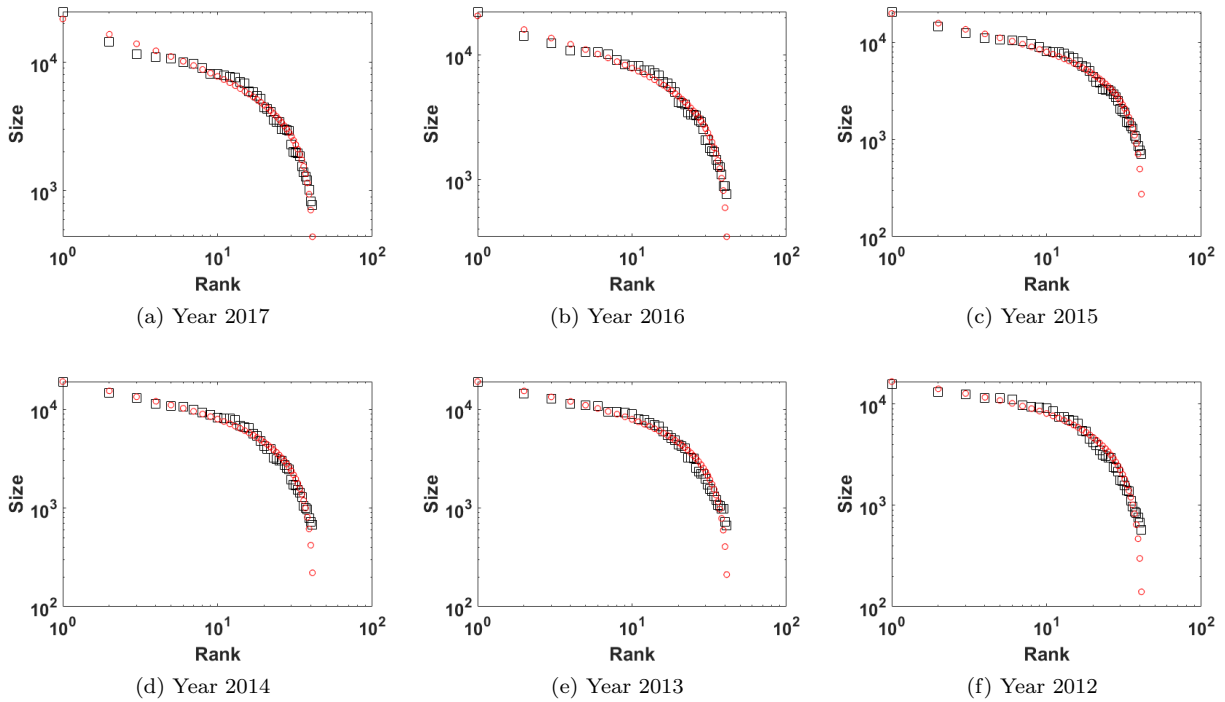


FIG. 10: Plots of actual (Black square) and predicted (Red circle) sizes over the rank for the personal income of USA

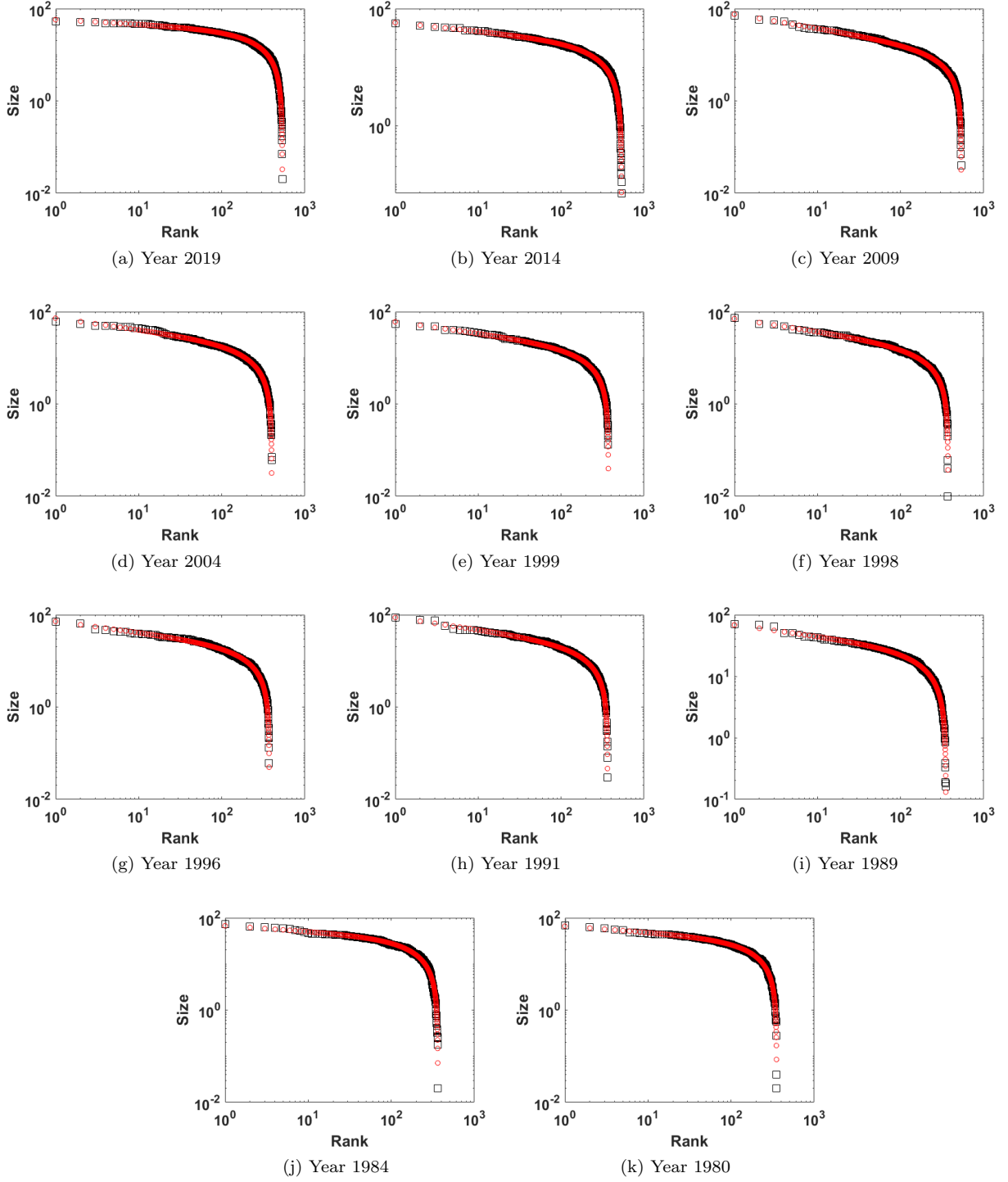


FIG. 11: Plots of actual (Black square) and predicted (Red circle) sizes over the rank for the percentage of vote-margin of Winners in Indian Lok Sabha Elections

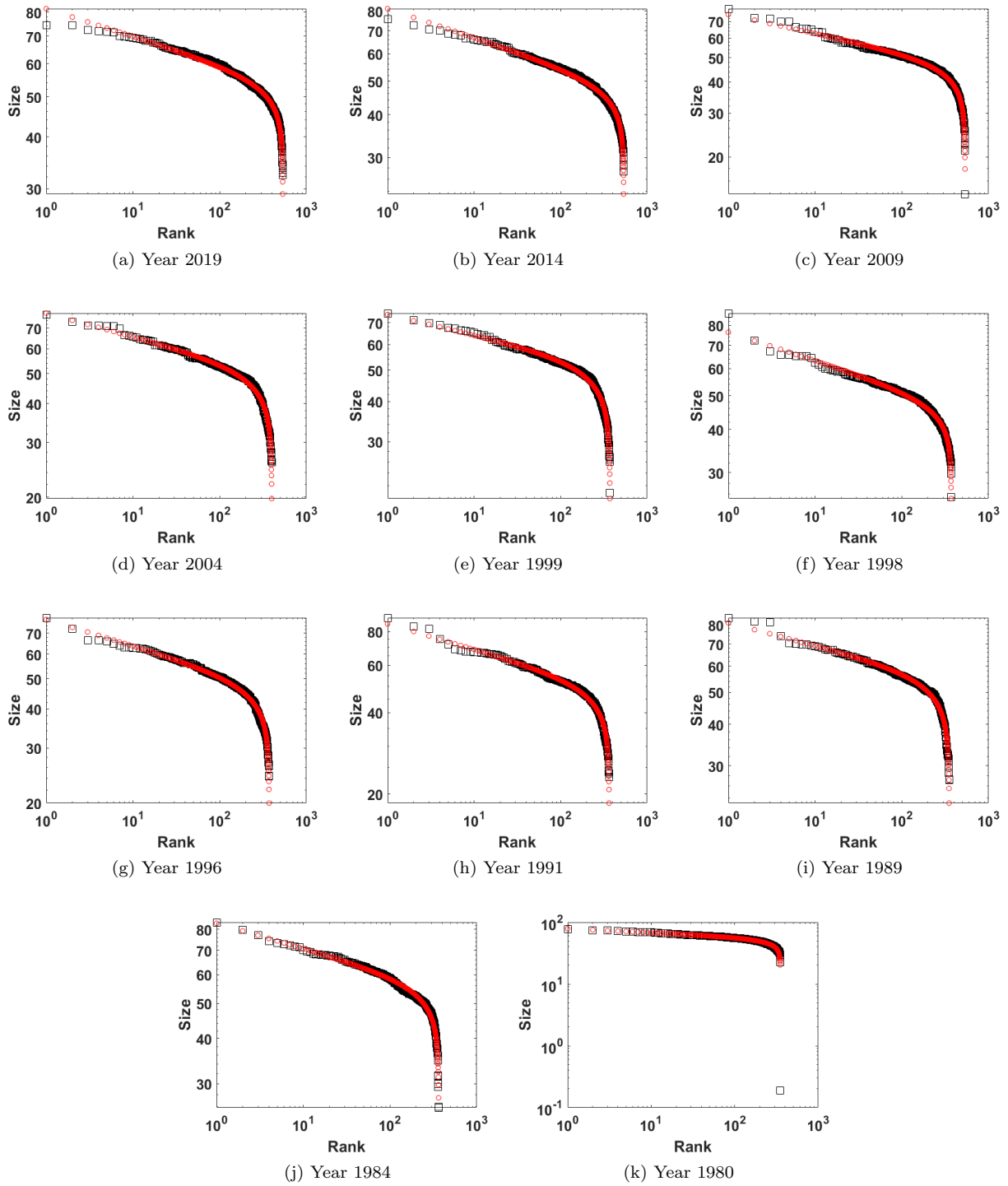


FIG. 12: Plots of actual (Black square) and predicted (Red circle) sizes over the rank for the Vote percentage of Winners in Indian Lok Sabha Elections

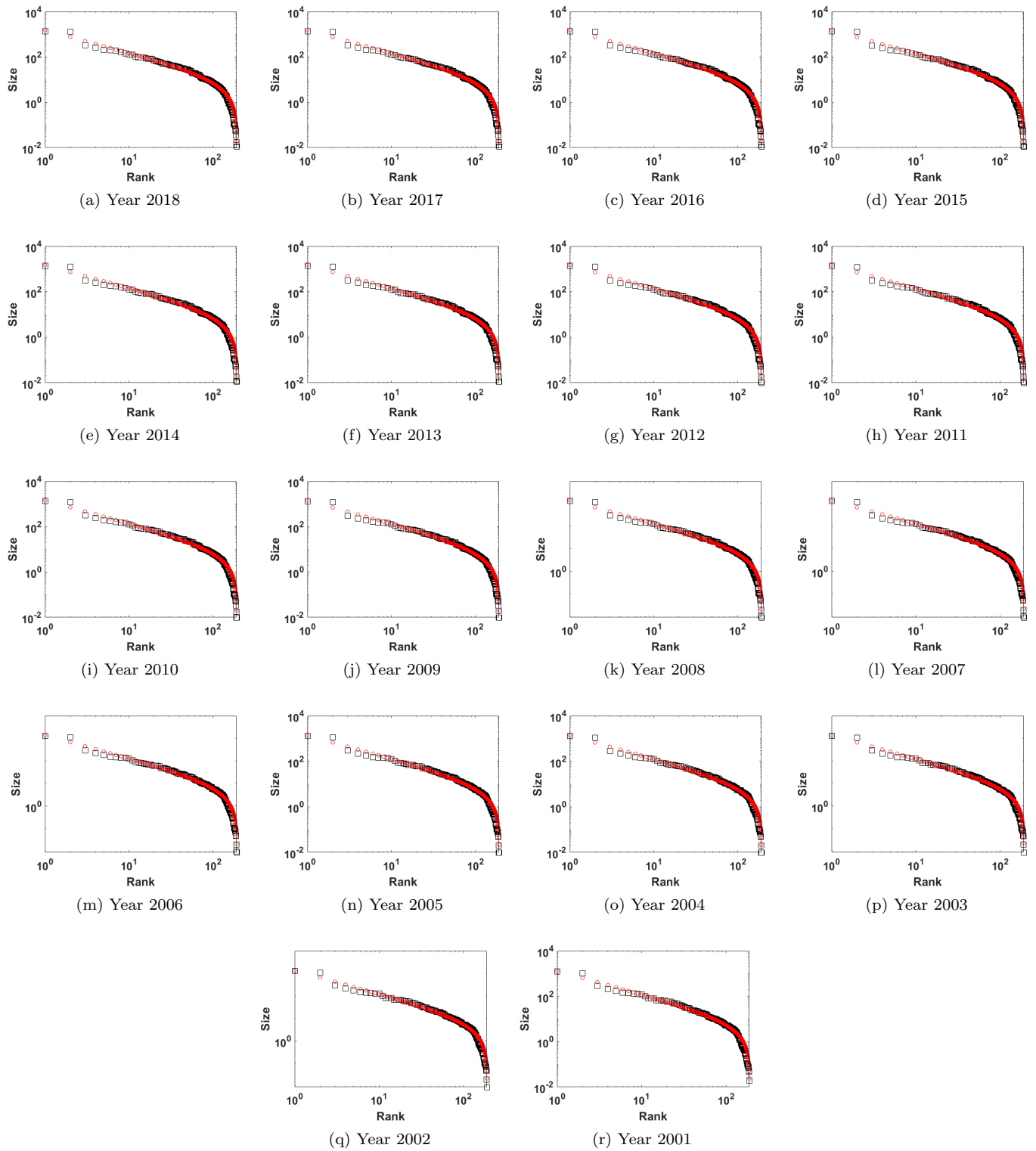


FIG. 13: Plots of actual (Black square) and predicted (Red circle) sizes over the rank for the population of different countries across the world

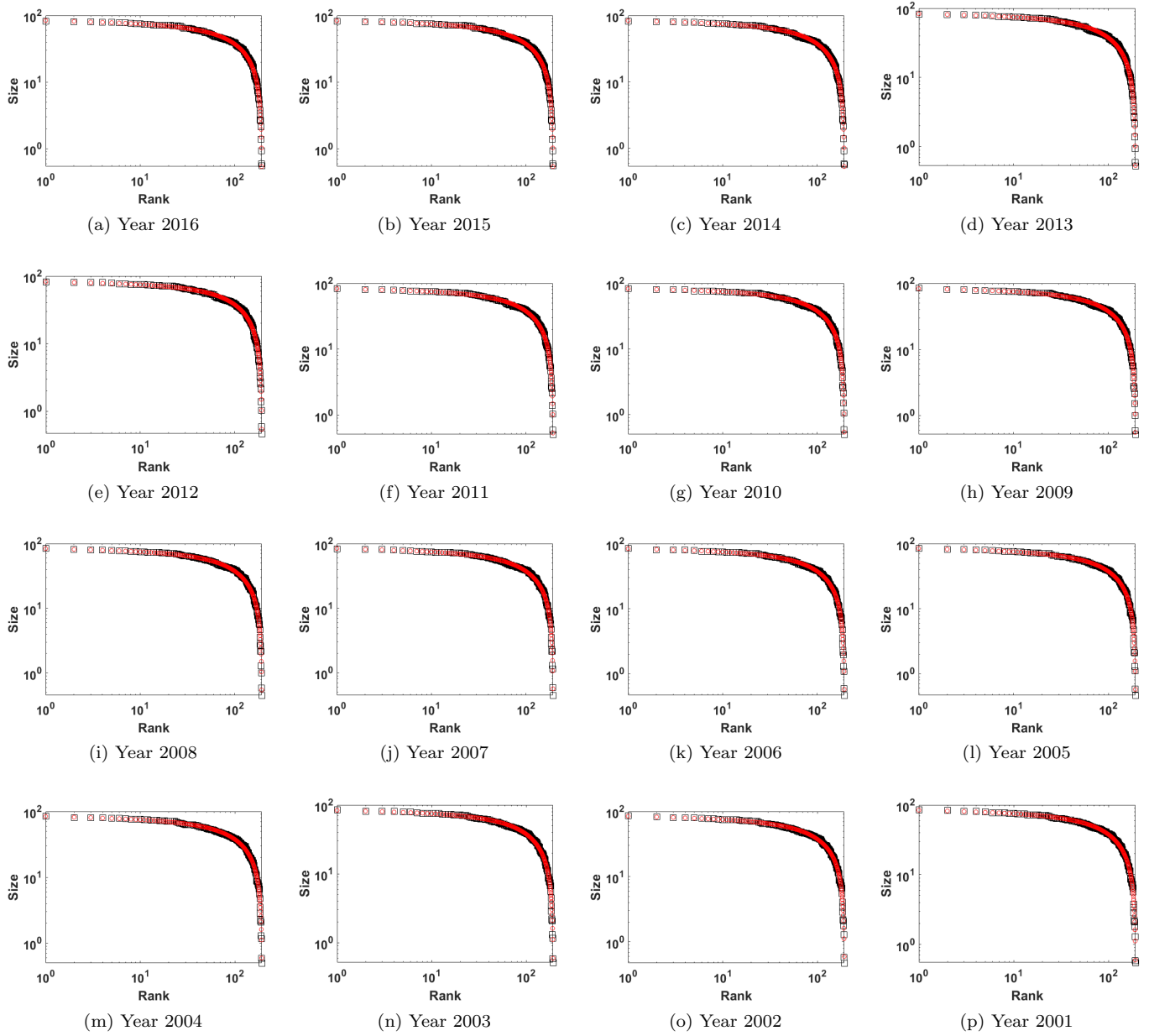


FIG. 14: Plots of actual (Black square) and predicted (Red circle) sizes over the rank for the agricultural land percentage of different countries across the world

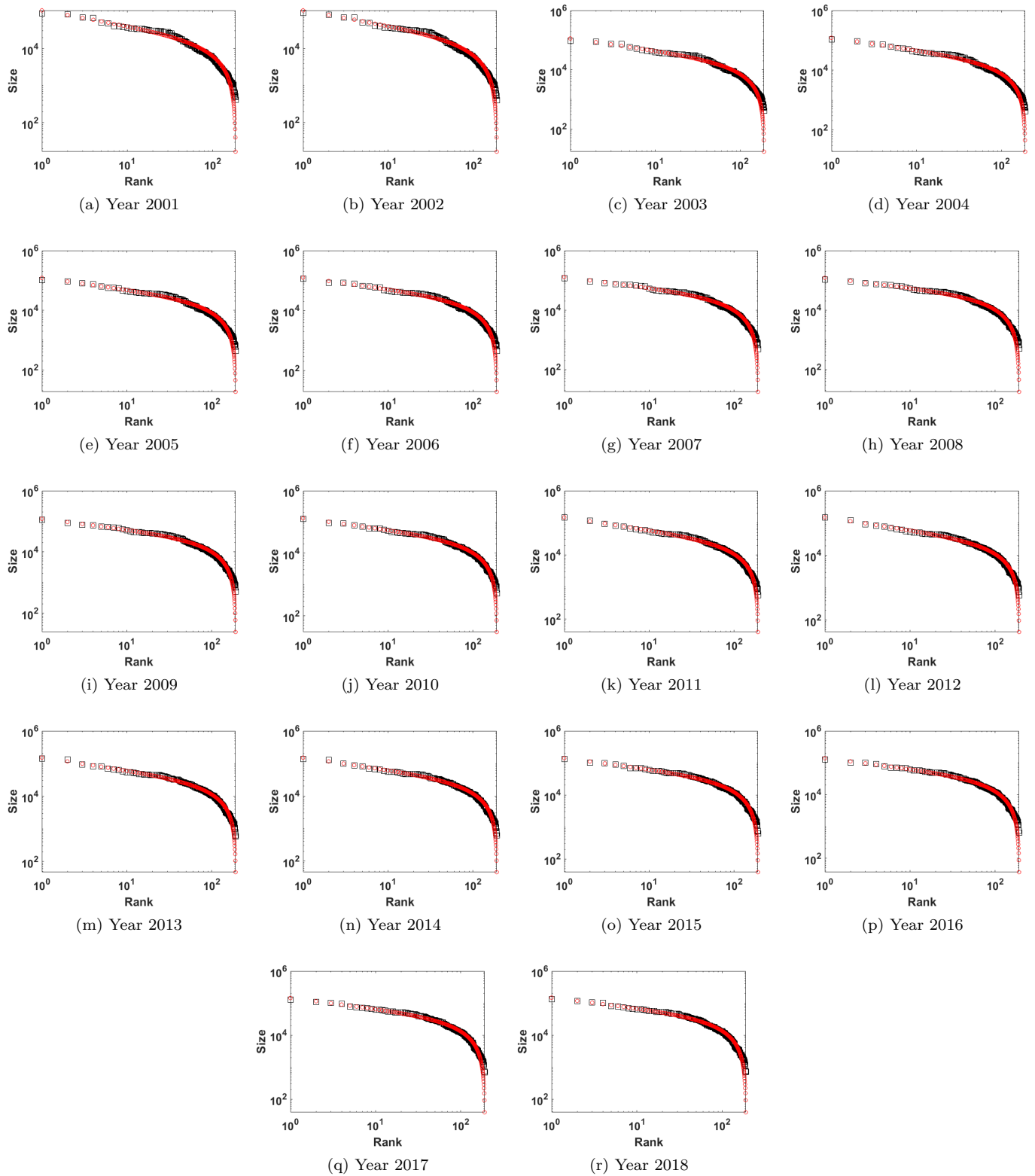


FIG. 15: Plots of actual (Black square) and predicted (Red circle) sizes over the rank for the per capita GDP of different countries across the world

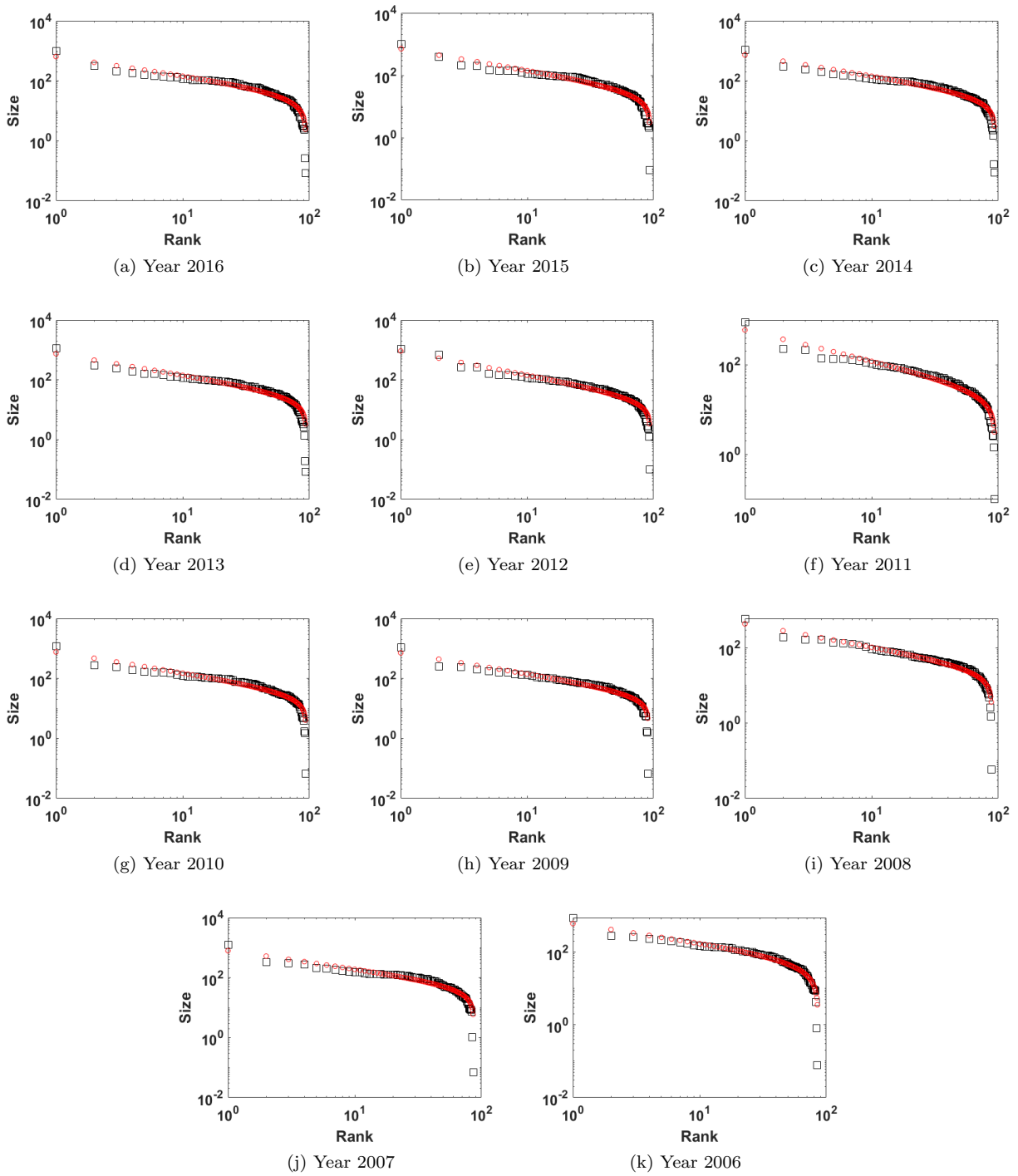


FIG. 16: Plots of actual (Black square) and predicted (Red circle) sizes over the rank for the Buffet indicator of different countries across the world